

SO₂–Faujasite Interaction: A Study by in Situ FTIR and Thermogravimetry

J. García-Martínez, D. Cazorla-Amorós,* and A. Linares-Solano

Departamento de Química Inorgánica, Universidad de Alicante, E-03080, Alicante, Spain

Received May 22, 2002. In Final Form: August 22, 2002

SO₂ adsorption and desorption on NaX and NaY zeolites, as a function of contact time and temperature, were studied combining in situ FTIR (diffuse reflectance with controlled chamber) and thermogravimetry. It is shown that SO₂ is physisorbed as a liquid on both zeolites at room temperature. Furthermore, SO₂ is chemisorbed on NaX, giving HSO₃⁻, which is transformed during the desorption treatment into S₂O₅²⁻. The presence of this species in this system has never been observed before by IR spectroscopy. Additionally, the geometry of the adsorbed species is discussed in detail. The SO₂ retention capacities of the zeolites was assessed by thermogravimetry and related to their porous structure. The different Si/Al ratios of both isostructure zeolites were found to be responsible for their different behaviors.

1. Introduction

Modified faujasites (X- and Y-type zeolites) have been studied as potential sorbents for sulfur dioxide due to their open structure, high pore volume (approximately 0.4 cm³/g¹) and large pore size (approximately 0.7 nm²). Besides this application, faujasites have been tested as SO₂ sensors³ and as catalyst for the Claus process, in which SO₂ and H₂S combine to form elemental sulfur.⁴ Additionally, the role of the SO₂ in the deNO_x process, usually catalyzed by zeolites, has been also studied.⁵

The interest of the SO₂–zeolite interaction can be noticed by the numerous papers devoted to its study. The first paper on this field was written in 1971⁴ and a few others in the following years.^{6–15} Karge et al.^{16–20} and Lavalley et al.^{21–26} have studied this system in a deep and

extensive way. Recently, some papers, mainly computational simulations, have been also published.^{27–29}

The main conclusions of these studies, carried out mainly by using IR spectroscopy, are that NaY at room temperature only physisorbs SO₂, showing a single band at 1320 cm⁻¹.^{4,18,20} On the other hand, NaX at room-temperature both physisorbs (band located at 1320 cm⁻¹) and chemisorbs SO₂ as HSO₃⁻ (bands at 1240 and 1080 cm⁻¹)^{9–12,20} and as S₂O₅²⁻. This latter species, formed only at high coverage, has never been observed by IR but only by UV–vis.²⁰

Our interest here focuses in a deeper characterization of the SO₂–faujasite interaction by using in situ FTIR spectroscopy at different temperatures. Additionally, the use of thermogravimetry will also allow us to quantify the formation of the different species and relate the SO₂ retention capacities of the studied zeolites to their porous properties. A better knowledge of the SO₂–zeolite interaction, especially of the nature and geometry of the different species involved, will allow a better use of zeolites in SO₂ applications.

2. Experimental Section

The zeolites used for this study, zeolites NaX (Si/Al = 5.0), and NaY (Si/Al = 9.6), were prepared by conventional hydrothermal synthesis as reported elsewhere.³⁰ The crystal size of these materials, determined by SEM, is in the range of 1 μm. A FTIR Nicolet 901–510P spectrometer with a diffuse reflectance device (Collector, SpectraTech) was used. This spectrometer has a controlled chamber (SpectraTech 0030–100). All the samples were treated under vacuum, heated, and reacted in situ while

* To whom correspondence should be addressed: Professor Diego Cazorla Amorós, Departamento de Química Inorgánica, Universidad de Alicante, E–03080, Alicante, Spain. Tel.: 96 590 3946. Fax: 96 590 3454. E-mail: cazorla@ua.es.

(1) García-Martínez, J.; Cazorla-Amorós, D.; Linares-Solano, A. *Studies in Surface Science Catalysis. Characterization of Porous Solids*; Unger, K. K., Kreysa, G., Baselt, J. P., Eds.; Elsevier: Amsterdam, 2000; Vol. 128, p 438–442.

(2) Meir, W. M.; Olson, D. H.; Baerlocher, Ch. *Atlas of Zeolite Structure Types*, 4th revised ed.; Elsevier: Amsterdam, 1996.

(3) Osada, M.; Sasaki, I.; Nishioka, M.; Sadakata, M.; Okubo, T. *Microporous Mesoporous Mater.* **1998**, *2*, 287.

(4) Slater, T. L.; Amberg, C. H. *Can. J. Chem.* **1972**, *50*, 3416.

(5) Iwamoto, M.; Mizuno, N.; Yahiro, H.; Taylor, K. C.; Blanco, J.; Nam, I. S.; Bartholomew, C. H.; Metcalfe, I. S.; Iglesia, E.; Sinev, M.; Duprez, D.; Amor, J.; Misono, M. *Stud. Surf. Sci. Catal., B* **1993**, *75*, 1285.

(6) Försted, H.; Schuldt, M. J. *J. Colloid Interface Sci.* **1975**, *52*, 380.

(7) Försted, H.; Schuldt, M. J. *Spectrochim. Acta* **1975**, *31A*, 685.

(8) Förster, H.; Seelemann, R. *J. Phys. Chem.* **1976**, *80*, 153.

(9) Ono, Y.; Suzuki, K.; Keii, T. *J. Phys. Chem.* **1974**, *78*, 218.

(10) Ono, Y.; Tokunaga, H.; Keii, T. *J. Phys. Chem.* **1975**, *79*, 752.

(11) Dudzik, Z.; Bilksa-Ziolek, M. *Bull. Acad. Pol. Sci., Ser. Sci. Chim.* **1975**, *23*, 699.

(12) Khulbe, K. C.; Mann, R. S.; Manoojian, A. *Zeolites* **1983**, *3*, 360.

(13) Datta, A.; Cavel, R. G.; Tower, R. W.; George, Z. M. *J. Phys. Chem.* **1985**, *89*, 443.

(14) Datta, A.; Cavel, R. G. *J. Phys. Chem.* **1985**, *89*, 450.

(15) Datta, A.; Cavel, R. G. *J. Phys. Chem.* **1985**, *89*, 454.

(16) Karge, H. G.; Raskó, J. *Proc. 3rd Int. Symp. Heterog. Catal.* **1975**, *615*.

(17) Karge, H. G.; Raskó, J. *J. Colloid Interface Sci.* **1978**, *64*, 522.

(18) Karge, H. G.; Ladebeck, J. *Proc. 5th Int. Conf. Zeolites* **1980**.

(19) Karge, H. G.; Ladebeck, J.; Nag, N. K. *7th Can. Symp. Catal.* **1980**.

(20) Karge, H. G.; Laniecki, M.; Ziolek, M. *Proc. 7th Int. Zeolite Conf.* **1986**.

(21) Lavalley, J. C.; Travert, J.; Chevreau, Th.; Lamotte, J.; Sau, O. *Chem Commun.* **1979**, 146.

(22) Lavalley, J. C.; Janin, A.; Preud'homme, J. *React. Kinet. Catal. Lett.* **1981**, *18*, 85.

(23) Saur, O.; Chevreau, Th.; Lamotte, J.; Travert, J.; Lavalley, J. C. *J. Chem. Soc., Faraday Trans. 1* **1981**, *77*, 427.

(24) Lavalley, J. C.; Lamotte, J.; Saussey, H.; Preud'homme, J. *Sulfur Lett.* **1982**, *1*, 101.

(25) Lavalley, J. C.; Lamotte, J.; Saur, O.; Mohammed Saad, A. B.; Tripp, C.; Morrow, B. A. *Proceedings of the International Conference on Fourier and Computerized Infrared Spectroscopy*; SPIE: Ottawa, 1985; Vol. 533, p 486.

(26) Lavalley, J. C.; Mohammed Saad, A. B.; Tripp, C. P.; Morrow, B. A. *J. Phys. Chem.* **1986**, *90*, 980.

(27) Srinivasan, A.; Grutzeck, M. W. *Environ. Sci. Technol.* **1999**, *33*, 1464.

(28) Nasluzov, V. A.; Shor, A. M.; Nortemann, F.; Staufer, M.; Yusanov, I. V.; Rosch, N. *J. Mol. Struct.—THEOCHEM* **1999**, *466*, 235.

(29) Marcu, I. C.; Sandalescu, I.; Gheorghie, G. *Rev. Roum. Chim.* **2000**, *45* (3), 243.

(30) García-Martínez, J. Thesis, Universidad de Alicante, 2000.

Table 1. Suggested Assignments of the IR Bands Observed during SO₂ Adsorption on NaY at 30 °C

wavenumber (cm ⁻¹)	assignment	wavenumber (cm ⁻¹)	assignment
3655	physisorbed SO ₂	1356	physisorbed SO ₂ , ν ₃
2516	physisorbed SO ₂ , ν ₁ + ν ₃	1190	SO ₂ (pyramidal), ν ₃ ^a
2470	physisorbed SO ₂ , ν ₁ + ν ₃	1120	physisorbed SO ₂ , ν ₁
2280	physisorbed SO ₂ , 2ν ₁	1050	SO ₂ (pyramidal), ν ₁ ^a
1650	physisorbed SO ₂		

^a SO₂ in IrCl(CO)(SO₂)(PPh₃).

the IR spectra were collected. The resolution used was 4 cm⁻¹, and 32 scans were collected for each spectrum.

All the samples were degassed in situ at 623 K in a vacuum. The reference spectrum was collected on the degassed sample at 303 K in He. IR spectra experiments were collected in the single beam mode at different times while a gas stream of 2500 ppm SO₂ in He was flowed over the sample at a flow rate of 6 mL/min. The flow rate was chosen deliberately small to be able to follow properly the evolution of the species on the surface of the zeolites.

A Stanton Redcroft 780 TG-DTA was used for the thermogravimetric experiments. The samples were first dehydrated at 400 °C (heating rate = 20 °C/min) and subsequently cooled at 30 °C and exposed to a flow of 2250 ppm of SO₂ in He at 90 mL/min. Finally, the samples were heated in He at 150 °C for 10 min in order to remove the weakly adsorbed SO₂ to distinguish the physisorbed from the chemisorbed SO₂. The pore volume of the zeolites were estimated by adsorption of CO₂ at 273 K as described elsewhere.¹ The density of the adsorbed phase was determined by dividing the final uptake of the SO₂ by the pore volume of the zeolite.

3. Results and Discussion

The SO₂ interaction with zeolite NaY at room temperature, as a function of the contact time, is shown in Figure 1, parts A and B. The adsorption of SO₂ on zeolite NaY produces nine different IR bands located at 3655, 2516, 2470, 2280, 1650, 1356, 1190, 1120, and 1050 cm⁻¹. The intensity of these bands increases with the adsorption time, except the band located at 2516 cm⁻¹ which remains constant (Figure 1B). Using data from the literature,^{19,20,23,31,32} most of these bands were assigned to the different vibrational modes of liquid SO₂, as shown in Table 1. The observation that the band located at 2516 cm⁻¹, which is due to gaseous SO₂,³¹ does not intensify while the others do suggests that SO₂ is adsorbed as a gas at short times until a certain concentration, above which it slowly condenses as a liquid.

This was corroborated by thermogravimetric experiments. The uptake of SO₂ on NaY at room temperature was found to be 267 mg of SO₂/g, while the micropore volume of this zeolite is 0.37 cm³/g,¹ giving a density of 0.72 g/cm³, which is similar to the liquid SO₂ density.³¹

To further corroborate this conclusion, in situ desorption experiments were performed by both IR (Figure 2) and thermogravimetry. All the IR bands decrease as the desorption temperature rises, observing no bands at 200 °C. Similarly, almost all the adsorbed SO₂ is removed after 10 min in He at 150 °C, confirming that NaY at 30 °C only physisorbs SO₂. This adsorption is presumably due to a specific and well-defined ion-dipole interaction (SO₂-Na⁺), as suggested by Kirik et al.³³ who using XRD showed that SO₂ is located 0.18 nm far away from the Na⁺. Additionally, both the high desorption temperature of the SO₂ physisorbed on NaY (desorption temperature = 117 °C) and the SO₂ uptake by NaY, which corresponds to

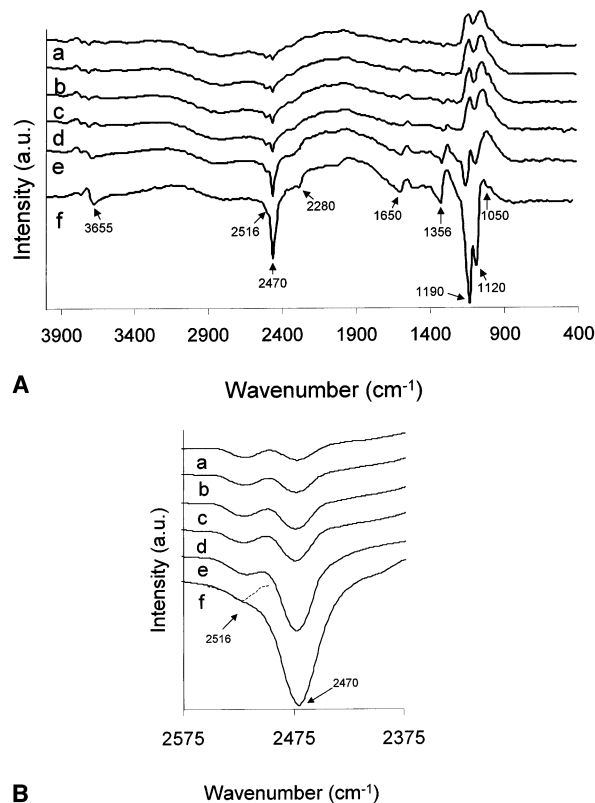


Figure 1. (A) IR spectra collected at different times during SO₂ adsorption on NaY at 30 °C: (a) 5, (b) 10, (c) 30, (d) 60, (e) 240, and (f) 360 min. (B) Detail of IR spectra collected at different times during SO₂ adsorption on NaY at 30 °C: (a) 5, (b) 10, (c) 30, (d) 60, (e) 240, and (f) 360 min.

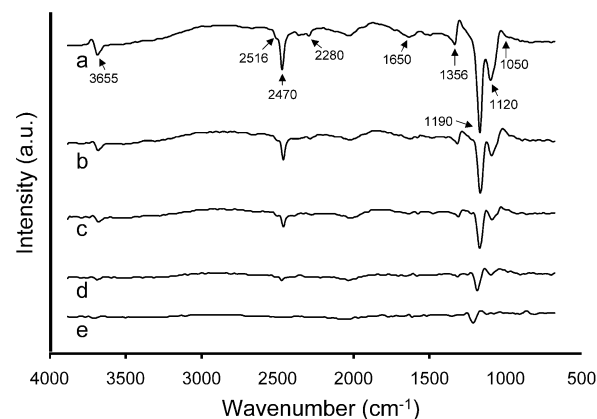


Figure 2. IR spectra collected at different temperatures after desorption of SO₂ from NaY (a) before desorption, (b) after 10 min at 100 °C, (c) after 10 min at 125 °C, (d) after 10 min at 150 °C, and (e) after 10 min at 200 °C.

0.955 mol of SO₂ per mole of Na⁺, are clear evidences of this specific ion-dipole interaction.

Finally, the IR experiments allowed us to learn about the geometry of the SO₂ adsorbed on NaY. Spectroscopic observations of different complexes, where SO₂ is present

(31) Nash, D. B.; Betts, B. H. *Icarus* **1995**, *117*, 402.

(32) Shor, A. M.; Rubaylo, A. I. *J. Mol. Struct.* **1997**, *410-411*, 133.

(33) Kirik, S. D.; Dubkova, A. A.; Sharonova, O. M.; Anshits, A. G. *Zeolites* **1992**, *292*, 12.

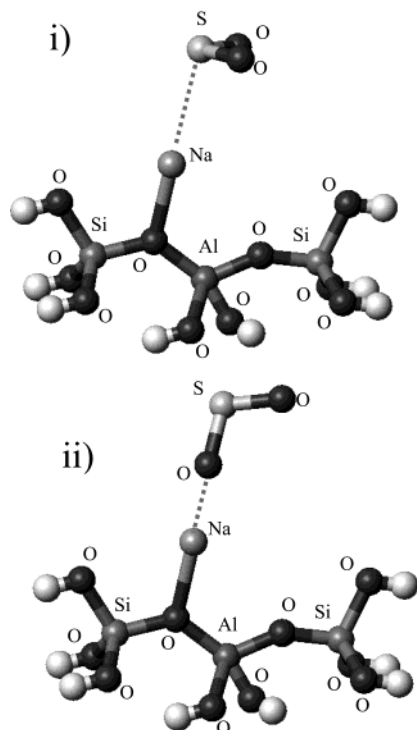


Figure 3. Model structures of SO_2 physisorbed on NaY: (i) pyramidal configuration and (ii) planar configuration.

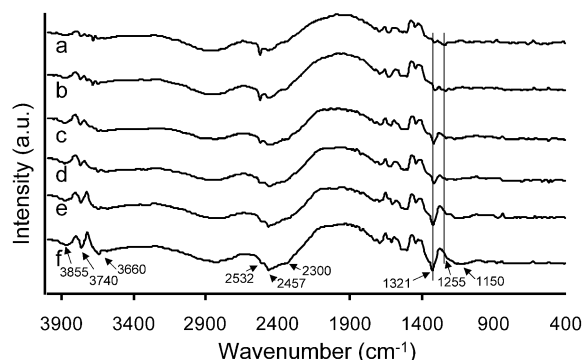


Figure 4. IR spectra collected at different times during SO_2 adsorption on NaX at 30 °C: (a) 2, (b) 5, (c) 15, (d) 60, (e) 90, and (f) 240 min.

as ligand, prove that SO_2 has two possible configurations. Thus, SO_2 in $\text{IrCl}(\text{CO})(\text{SO}_2)(\text{PPh}_3)$ interacts with the cation through the central sulfur atom, in a pyramidal configuration, producing two bands located at 1198–1185 and 1049 cm^{-1} ,³⁴ very close to those observed when SO_2 is adsorbed on NaY (i.e., at 1190 and 1050 cm^{-1}). Additionally, SO_2 can interact to the cation through one of the oxygens as it does in $\text{SbF}_5(\text{SO}_2)$, producing two bands located at 1356 and 1120 cm^{-1} ,³⁵ also observed in SO_2 adsorbed on NaY, at 1327 and 1102 cm^{-1} . Thus, physisorbed SO_2 on NaY shows two different configurations, as shown in Figure 3. In both of them, SO_2 is oriented to the Na^+ : (i) through the central sulfur atom, giving a pyramidal geometry, and (ii) through one of the oxygens, in a flat configuration.

The adsorption of SO_2 on NaX as a function of contact time was also studied by FTIR, as is shown in Figure 4. In this case, eight bands were observed (3855, 3660, 2532,

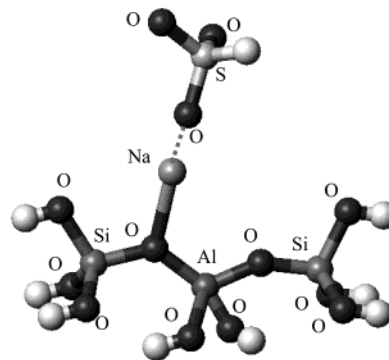


Figure 5. Model structure of HSO_3^- chemisorbed on NaX showing a pyramidal configuration.

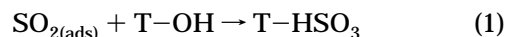
Table 2. Suggested Assignments of the IR Bands Observed during SO_2 Adsorption on NaX at 30 °C

wavenumber (cm^{-1})	assignment	wavenumber (cm^{-1})	assignment
3855	SiO–H	2300	physisorbed SO_2
3740	SiO–H	1321	physisorbed SO_2
3660	SiO–H	1255	H– SO_3^-
2532	H– SO_3^-	1150	physisorbed SO_2
2457	physisorbed SO_2	1050	$\text{S}_2\text{O}_5^{2-}$

2457, 2300, 1321, 1255, 1150 cm^{-1}) and also most of them increase with time, but not those located at 2532 and 1255 cm^{-1} . Similar to the previous case, some bands (those located at 2457, 2300, 1321, and 1150 cm^{-1}) were assigned to liquidlike physisorbed SO_2 ,³¹ as shown in Table 2, which includes the suggested assignments of all the bands. Again, thermogravimetry gives a density for adsorbed SO_2 of 0.75 g/cm^3 , close to the liquid SO_2 density.³¹

However, contrary to the zeolite NaY, not all the bands could be assigned to physisorbed SO_2 . Thus, the bands located at 3855 and 3660 cm^{-1} were related to the perturbation of the SiO–H and AlO–H bonds by the SO_2 through hydrogen bonding. Karge et al. related this observation with the SiOH– SO_2 interaction.¹⁹ The same kind of interaction was reported in the case of SO_2 adsorbed on silica.³⁶ Finally, there are two bands located to 2532 and 1255 cm^{-1} due to chemisorbed SO_2 in the form of HSO_3^- , which existence was proposed by Karge et al.¹⁹ The observation that the band located at 2532 cm^{-1} does not disappear after heat treatment in He at 300 °C suggests that this band is due to HSO_3^- and not to physisorbed SO_2 which shows a band at 2516 cm^{-1} . The band at 2532 cm^{-1} corresponds to the H stretching in the HSO_3^- ,³⁷ suggesting that its sulfur atom is, at least, partially protonated, giving a C_{3v} pyramidal configuration, as shown in Figure 5.

A remarkable observation from Figure 4 is that the bands due to the OH terminal groups and physisorbed SO_2 show similar behavior; i.e., the intensity of the bands related to both species increases with time. This suggests that the SO_2 interaction with the hydroxyls and the formation of HSO_3^- is intimately related, as was also reported by other authors^{13,14,36,38} who proposed the following reaction:



The fact that the AlO–H bond is weaker than the SiO–H one³⁹ can help to explain the formation of HSO_3^- on NaX

(34) Vaska, L.; Bath, S. S. *J. Am. Chem. Soc.* **1966**, *88*, 1333.

(35) Moore, J. W.; Baird, H. W.; Miller, H. B. *J. Am. Chem. Soc.* **1968**, *90*, 1358.

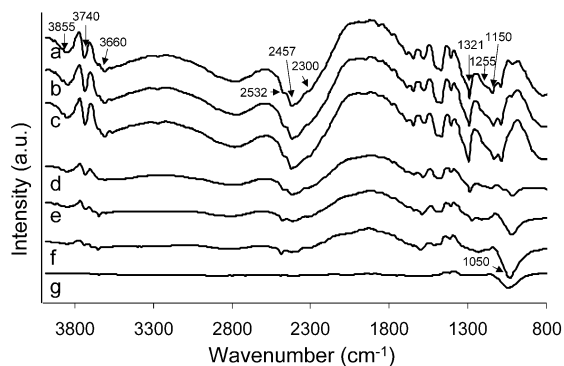
(36) Ma, Y. H.; Roux, A. J. *AIChE J.* **1973**, *19*, 1055.

(37) Miller, F. A.; Wilkins, C. H. *Anal. Chem.* **1952**, *24*, 1253.

(38) Saussey, H.; Valley, A.; Lavalley, J. C. *Mater. Chem. Phys.* **1983**, *9*, 457.

Table 3. Suggested Assignments of the IR Bands Observed during SO₂ Adsorption on NaY at 180 °C

wavenumber (cm ⁻¹)	assignment	wavenumber (cm ⁻¹)	assignment
3714	SiO-H	1844	HSO ₃ ⁻ , ν _{S=O} antis + δ _{SO₂} sim
3642	SiO-H	1772	HSO ₃ ⁻ , δ _H SO + δ _{SO₂} sim
2928	H-SO ₃ ⁻	1712	HSO ₃ ⁻ , ν _{S=O} antis + δ _{SO₂} antis
2858	H-SO ₃ ⁻	1189	H-SO ₃ ⁻ , ν _{S=O} antis
2472	physisorbed SO ₂	1123	H-SO ₃ ⁻ , δ _H SO

**Figure 6.** IR spectra collected at different temperatures after desorption of SO₂ from NaX (a) before desorption, (b) after 10 min at 100 °C, (c) after 10 min at 150 °C, (d) after 10 min at 200 °C, (e) after 10 min at 250 °C, (f) after 10 min at 300 °C, and (g) after 10 min at 400 °C.

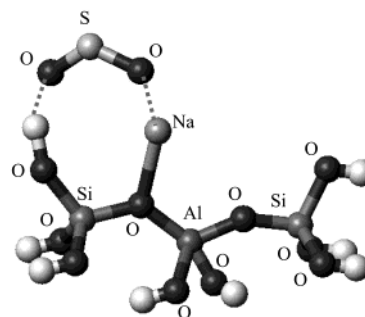
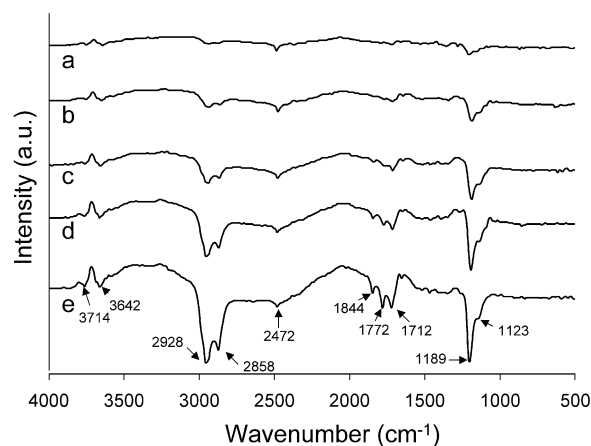
and not on NaY, which has the same structure but a higher Si/Al ratio (NaX, Si/Al = 5.0, and NaY, Si/Al = 9.6).³⁹ A further evidence of the influence on the Al content in the SO₂-faujasite interaction is that dealuminated zeolite Y (even with higher Si/Al ratio than NaY) also exclusively physisorbs SO₂.³²

The formation of chemisorbed species was confirmed by in situ desorption IR experiments, shown in Figure 6. The bands related to physisorbed SO₂ (those located at 2457, 2300, 1321, and 1150 cm⁻¹) disappear completely at a relatively low temperature, approximately at 200 °C, but those which were related to HSO₃⁻ require higher temperatures, 300 °C. Moreover, the disappearance of these bands occurs simultaneously to the appearance of a new band located at 1050 cm⁻¹, a characteristic band of S₂O₅²⁻.³⁹ This observation suggests that HSO₃⁻ does not desorb, but it is transformed into a new species during heat treatment (S₂O₅²⁻). Previous studies suggested the formation of S₂O₅²⁻ at high coverage by condensation of HSO₃⁻ molecules;²⁰ however, its existence was not proved by IR before.

The interaction of one of the oxygens of the SO₂ with the Na⁺ (bands at 1321 and 1150 cm⁻¹) and of the other one with the OH terminal groups (bands at 3855 and 2660 cm⁻¹) may produce a cyclic structure shown in Figure 7 which favors the reaction of SO₂ with OH groups to form HSO₃⁻.

These conclusions were corroborated by thermogravimetry. The SO₂ retention capacity of NaX at room temperature was found to be 276 mg of SO₂/g of zeolite, slightly higher than that of NaY. However, in NaX only 84% of SO₂ is removed after heat treatment at 150 °C, which confirms the presence of chemisorbed species.

Finally, the SO₂ adsorption on NaY was also studied at 180 °C in order to investigate the formation of chemisorbed species on this zeolite. The evolution of the IR spectra of NaY treated on SO₂ at 180 °C is shown in Figure 8. In this

**Figure 7.** Model structure of SO₂ physisorbed on NaX showing a cyclic configuration.**Figure 8.** IR spectra collected at different times during SO₂ adsorption on NaY at 180 °C: (a) 2, (b) 10, (c) 30, (d) 60, and (e) 180 min.

case, 10 different bands are observed, located at 3714, 3642, 2928, 2858, 2472, 1844, 1772, 1712, 1189, and 1123 cm⁻¹, for which the suggested assignment is compiled in Table 3. Again, almost all of them intensify with adsorption time. Only a weak band located at 2472 cm⁻¹ remains constant.

All these bands can be related to three different species: (i) perturbed OH terminals groups (bands located at 3714 and 3642 cm⁻¹), (ii) gaseous SO₂ (weak band located at 2472 cm⁻¹), and (iii) HSO₃⁻ (bands located at 2928, 2858, 1844, 1772, 1712, 1189, and 1123 cm⁻¹).

The two bands located 2928 and 2858 cm⁻¹ are related to H-S stretching in HSO₃⁻,³⁷ which must be in a C_{3v} pyramidal configuration, such as that shown in Figure 5 for NaX at room temperature. However, the bands located at 1189 and 1123 cm⁻¹ must be related to the antisymmetric stretching of the S=O bond and the bending of the H-S=O bond present in the HSO₃⁻ in the planar geometry³⁷ shown in Figure 9, which was not detected for NaX.

In situ IR desorption experiments done at 180 °C in He at different times (shown in Figure 10) corroborate that the band located at 2472 cm⁻¹ is due to gaseous SO₂, which is the only band that disappears after permutation to He. Moreover, the SO₂ retention capacity of NaY at 180 °C is

(39) Barrer, R. M. *Zeolites and Clay Minerals*; Academic Press: London, 1978.

(40) Kirik, S. D.; Dubkova, A. A.; Sharonova, O. M.; Anshits, A. G. *Zeolites* **1992**, 292, 12.

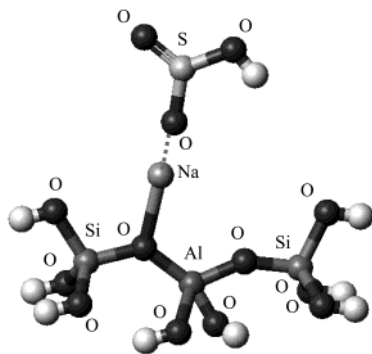


Figure 9. Model structure of HSO_3^- chemisorbed on NaY showing a planar configuration.

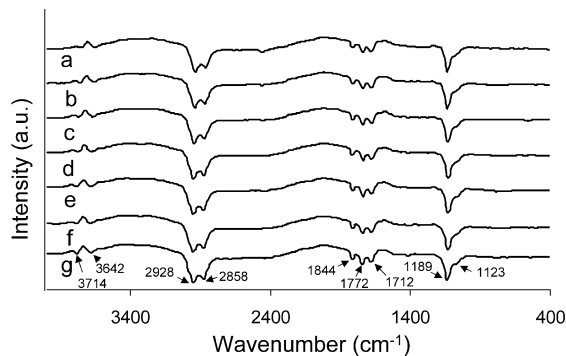


Figure 10. IR spectra collected at different times at 180 °C after desorption of SO_2 from NaY: (a) before desorption and (b) after 5, (c) 10, (d) 20, (e) 30, (f) 40 min, and (g) 60 min at 400 °C.

54 mg of SO_2/g , significantly lower than that at room temperature, which is not desorbed even after a heat treatment at 600 °C.

4. Conclusions

The combination of in situ IR spectroscopy and thermogravimetry allowed us not only to identify the chemical species formed during SO_2 –faujasite interaction, but also

to identify the aggregation state of the adsorbed phase, the thermal stability of the different species formed, their geometry, and a new species, $\text{S}_2\text{O}_5^{2-}$, whose presence was proposed but never observed by IR spectroscopy before. The configuration of the different species adsorbed was based on the comparison with IR spectra of metal complexes where SO_2 is present with different orientations and distinctive bands of HSO_3^- with different conformations appear.

The study of the SO_2 –faujasite interaction by in situ IR spectroscopy and thermogravimetry leads us to the following conclusions:

(a) SO_2 is physisorbed on NaY at room temperature mainly as a liquid, through an ion–dipole interaction with the Na^+ cation in a $\text{SO}_2:\text{Na}^+$ molar ratio close to 1, orienting either the central sulfur atom or one of its two oxygens to the Na^+ , originating two different configurations.

(b) In the case of the zeolite NaX at room temperature, one of the two oxygen atoms of physisorbed SO_2 is oriented to the Na^+ (ion–dipole interaction) while the other is hydrogen bonded to the OH terminal groups of the zeolite. Additionally, the rest of the SO_2 is chemisorbed as HSO_3^- in a C_{3v} pyramidal configuration, which is transformed into $\text{S}_2\text{O}_5^{2-}$ during heat treatment.

(c) SO_2 is almost exclusively chemisorbed on NaY at 180 °C as HSO_3^- , showing both pyramidal and planar configurations.

The fact that SO_2 is weakly adsorbed on NaY zeolite points out the suitability of this material for applications where SO_2 must be removed gently (regenerable SO_2 -capture systems) or where SO_2 poisoning could be a problem (i.e., deNOx catalyst). Finally, the influence of the Si/Al ratio for a given zeolite structure on the formation of chemically adsorbed SO_2 could also be a useful tool for the interpretation of SO_2 adsorption on other aluminosilicates.

Acknowledgment. The authors thank the DGICYT (Project MAT2000-0621) for financial support. J.G.M. thanks the MEC for the Ph.D. Thesis fellowship.

LA020483F